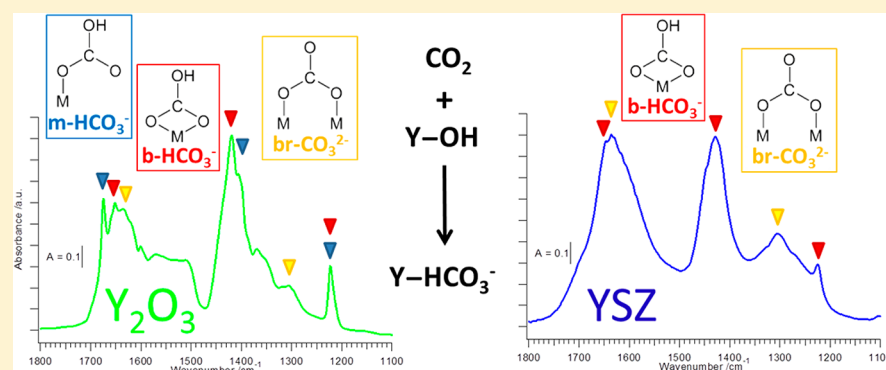# In Situ FT-IR Spectroscopic Study of CO_2 and CO Adsorption on Y_2O_3, ZrO_2, and Yttria-Stabilized ZrO_2

Eva-Maria Köck, Michaela Kogler, Thomas Bielz, Bernhard Klötzer, and Simon Penner*

Institute of Physical Chemistry, University of Innsbruck, Innrain 52a, A-6020 Innsbruck, Austria

S *Supporting Information*

ABSTRACT: In situ FT-IR spectroscopy was exploited to study the adsorption of CO_2 and CO on commercially available yttria-stabilized ZrO_2 (8 mol % Y, YSZ-8), Y_2O_3, and ZrO_2. All three oxides were pretreated at high temperatures (1173 K) in air, which leads to effective dehydroxylation of pure ZrO_2. Both Y_2O_3 and YSZ-8 show a much higher reactivity toward CO and CO_2 adsorption than ZrO_2 because of more facile rehydroxylation of Y-containing phases. Several different carbonate species have been observed following CO_2 adsorption on Y_2O_3 and YSZ-8, which are much more strongly bound on the former, due to formation of higher-coordinated polydentate carbonate species upon annealing. As the crucial factor governing the formation of carbonates, the presence of reactive (basic) surface hydroxyl groups on Y-centers was identified. Therefore, chemisorption of CO_2 most likely includes insertion of the CO_2 molecule into a reactive surface hydroxyl group and the subsequent formation of a bicarbonate species. Formate formation following CO adsorption has been observed on all three oxides but is less pronounced on ZrO_2 due to effective dehydroxylation of the surface during high-temperature treatment. The latter generally causes suppression of the surface reactivity of ZrO_2 samples regarding reactions involving CO or CO_2 as reaction intermediates.

1. INTRODUCTION

Yttria-stabilized ZrO_2 (YSZ) is already commonly used as a solid oxide fuel cell (SOFC) electrolyte and anode component.[1] However, despite its technological importance, YSZ itself is a very complex material, adopting different crystal structures (monoclinic, tetragonal, and cubic) with varying Y content below 20 mol %.[2] Of all the associated mixed oxide compounds, YSZ containing 8 mol % yttria is the most technologically important one. Therefore, on the one hand, the understanding of molecular processes on its surface is highly desirable, and on the other hand, insights into the surface reactivity of YSZ are also expected from in-depth studies of the two chemical constituents of the YSZ structure, that is, Y_2O_3 and ZrO_2. The aim for a better understanding of the surface chemistry of the latter two oxides is also fueled by their technological relevance, comprising the use as ceramic materials or as catalysts for a number of chemical reactions.[3,4] However, despite their importance, the use of YSZ and ZrO_2 strongly depends on the particular polymorph used. The most common modification of ZrO_2 is the monoclinic structure that is the only thermodynamically stable phase until ~1400 K, where a phase change to a tetragonal modification takes place. Above a temperature of ~2600 K a cubic structure is present.[4] These polymorphic forms exhibit strikingly different chemical properties, giving rise to also different catalytic behavior. The tetragonal and the cubic phases are catalytically more active than their monoclinic counterpart.[5] Doping ZrO_2 with Y_2O_3 stabilizes either the cubic or tetragonal phase (strongly depending on production technique) over a large temperature range and creates oxygen vacancies.[2,3] Thus, a lot of progress has been made especially regarding characterization of the surface chemistry of a variety of different ZrO_2 samples. Materialwise, this essentially refers to supported metal/oxide systems[6−9] and sulfated ZrO_2 samples.[7,10] Most data are available for pure ZrO_2, with the exception of comparative adsorption studies of tetragonal and monoclinic ZrO_2.[10−13] Strikingly different, information on the surface chemistry of Y_2O_3 and YSZ mixed oxide phases is virtually nonexistent, and

adsorption studies essentially represent no-man's land. Information on Y_2O_3 is restricted to FT-IR studies of supported Ru and Pd/Y_2O_3 systems and Er-doped Y_2O_3, being used as transparent ceramics.[14] Studies on YSZ by FT-IR spectroscopy are almost exclusively focused on investigating its crystal structure. One notable exception in that respect is the studies on ZrO_2, doped with 3 mol % yttria, which usually serves as a compound to simulate tetragonal ZrO_2.[10]

The aim of our studies therefore is to provide a first comparison of the surface chemical properties of technically used YSZ with 8 mol % yttria content and its separated chemical constituents Y_2O_3 and ZrO_2. As representative probe molecules, CO and CO_2 were chosen, due to their importance as reactants in a variety of chemical reactions, including the water−gas shift reaction or other C1 reactions relevant to anodic fuel conversion in solid oxide fuel cells. As the perfect method for monitoring the adsorbed species under technically relevant conditions, a dedicated in situ FT-IR spectroscopy setup was used, allowing static and flowing treatments up to the bar range and elevated temperatures up to 773 K. Exceeding the scientific input from the simple comparison between the three oxidic materials, we also anticipate in-depth information on the reactivity of more complex reactions and materials. Special attention was also paid to a comparison of the determined surface reactivity to literature data, as especially oxide pretreatments are expected to strongly alter the adsorption behavior. Regarding surface studies on oxides, this essentially refers to the hydroxylation state of the surface.

2. EXPERIMENTAL SECTION

2.1. Materials. Commercial powders of Y_2O_3, ZrO_2, and YSZ were used as starting materials. Cubic (bcc) Y_2O_3 (yttrium(III)oxide, nanopowder, <50 nm particle size) and tetragonal YSZ (zirconium(IV)oxide-yttria stabilized, nanopowder, containing 8 mol % Y_2O_3 as stabilizer, from now on called "YSZ-8") were supplied by Sigma Aldrich and monoclinic ZrO_2 (with a small amount of tetragonal phase after thermal annealing at 1173 K, zirconium(IV)oxide, 99.978%) by Alfa Aesar. All samples were pretreated by calcination at 1173 K in air and subsequently checked by XRD for structural changes upon annealing. The surface area after pretreatment was determined by nitrogen adsorption at 77 K according to the BET method as 21.7 m^2/g (Y_2O_3), 31.6 m^2/g (YSZ-8), and 10.4 m^2/g (ZrO_2). For BET measurements, a Quantachrome Nova 2000 Surface Area and Pore Size Analyzer was used. Gases were supplied by Messer (CO_2 4.5 and CO 4.7).

2.2. FT-IR Studies. FT-IR spectra were recorded in transmission mode on a Perkin-Elmer FT-IR System 2000 spectrometer. The powder samples were pressed into thin pellets using a pressure of 2 t (sample mass about 100 mg each). The pellets were subsequently placed inside a home-made in situ reactor cell. The path length of the IR reactor cell amounts to 20 cm. This cell setup allows treatments under static and flowing conditions up to pressures of 1 bar and temperatures up to 873 K. The temperature is controlled by a thermocouple placed next to the pellet. Pretreatment of the powders was performed outside the cell (annealing up to 1173 K), and the pellet was mounted hot into the IR cell. Vacuum was applied immediately (10^{-6} mbar). Calcium fluoride is used as window material allowing access to wavelength ranges above 1000 cm^{-1}. To ensure identical starting conditions, samples were oxidized with 20% oxygen seeded in helium at 873 K for

one hour. To ensure a minimal degree of hydroxylation, during the flow mode measurements the gases are cleaned and dried using two liquid nitrogen or liquid nitrogen/ethanol cooling traps. Flowing measurements were performed under ambient conditions. In static mode, the gases are preadsorbed on a 5 Å zeolite trap binding water sufficiently strongly, before the dry gases are desorbed into the evacuated and degassed cell. All reported spectra are corrected with the spectrum of the dry preoxidized oxide pellet prior to adsorption.

3. RESULTS AND DISCUSSION

3.1. CO₂ Adsorption. *3.1.1. Y_2O_3.* Figure 1 shows an overview of effects associated with the static adsorption of dry CO_2 on Y_2O_3 at room temperature using CO_2 pressures up to 10 mbar.
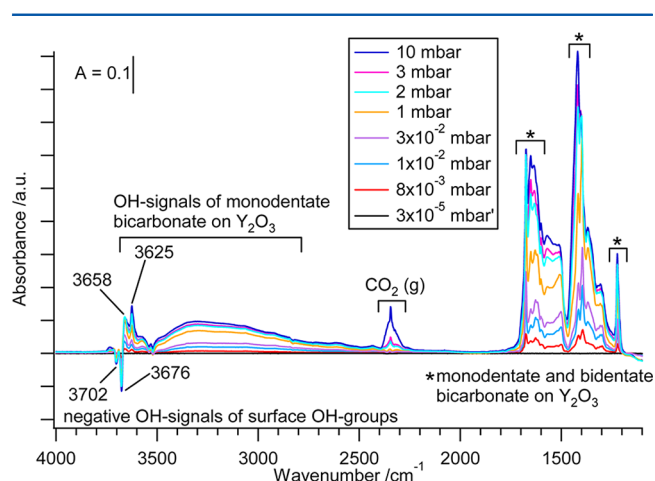

Figure 1. Infrared spectra of static adsorption of CO_2 on pure Y_2O_3 at room temperature at pressures up to 10 mbar.

As it can be clearly seen, the adsorption leads to formation of a number of distinct (bi)carbonate and hydroxyl species. The assignment of the carbonate species (detailed representation in Figure 3) was based on recent investigations on carbonate formation on different Ga_2O_3 polymorphs,[15] where both experimental and theoretical information is most abundant and thus the assignment in the present case is most straightforward. The structure of the most likely analogous (bi)carbonate species[15] is highlighted in Figure S1 (Supporting Information).

A closer look at Figure 3 reveals that at a pressure of 3×10^{-5} mbar almost no formation of carbonates is observed, whereas raising the pressure up to 1 mbar leads to the formation of a dominant species with signals at 1674, 1397, and 1223 cm^{-1}. During further pressure increase to 10 mbar, another species with signals at 1652, 1419, and 1223 cm^{-1} dominates the spectra. On the basis of ref 15, these peaks can be attributed to the ν_{as}, ν_s, and δ_{OH} vibration modes of monodentate and bidentate bicarbonates. The intensification of the latter peaks correlates with the decrease of signals at 3702 and 3676 cm^{-1} and an increase of the associated modes at 3658 and 3625 cm^{-1} (Figures 2 and 3).

Figure 2 shows that, according to refs 16 and 17, the negative peaks are related to $\nu(OH)$ modes of isolated surface hydroxyl groups of the oxide (more than one peak is visible due to the presence of differently coordinated hydroxyl groups), which become consumed by bicarbonate formation, and the
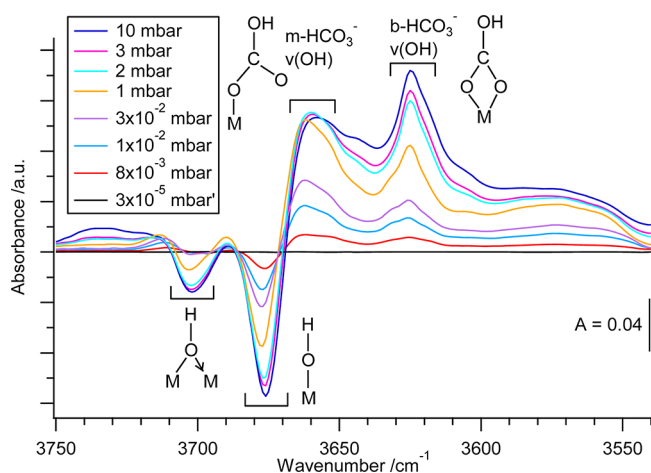
Figure 2. Details of the room-temperature-collected infrared spectra of adsorbed CO_2 on Y_2O_3 shown in Figure 1 in the wavenumber range between 3750 and 3540 cm^{-1} at pressures up to 10 mbar in the region of the hydroxyl stretching modes.
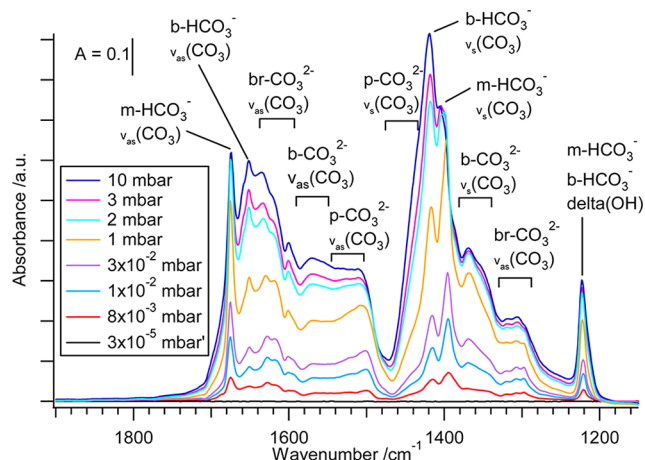

Figure 3. Assignment of the infrared signals between 1900 and 1160 cm^{-1} of the observed (bi)carbonates on Y_2O_3 at room temperature at pressures up to 10 mbar.

accordingly positive signals can be associated with the $\nu(OH)$ modes of the newly formed hydroxyl groups of the bicarbonates. The intensity of the hydroxyl group at 3658 cm^{-1} correlates with the rise of the signals of the monodentate bicarbonate, whereas the signal at 3625 cm^{-1} matches the bidentate bicarbonate species. The analogous appearance of two different bicarbonate species was also observed on ceria samples.[17] The broad feature below 3500 cm^{-1} can be assigned to interacting hydroxyl groups of the formed bicarbonates. Hence, the main process associated with chemisorption of a CO_2 molecule on Y_2O_3 is the insertion into a basic surface hydroxyl group leading to the formation of bicarbonates. Note that the experiments probably do not represent true thermodynamically equilibrated processes since the waiting time to reach an adsorption equilibrium had to be balanced against possible contamination of the surface especially at prolonged times.

Following refs 15 and 18 the assignment to the different (bi)carbonate species is shown in Figure 3. Concerning the pattern of the peaks it is apparent that with increasing coordination of the (bi)carbonates a superposition of signals of the different adsorbed features occurs. As pointed out in ref 19

such an effect is due to the presence of different adsorption sites arising from different coordination of the metal atoms on the surface, especially on a powder sample. Also an interaction between different adsorbed species can not be excluded.[20]

To test the thermal stability of the adsorbates, Figure 4 illustrates the thermal evolution of the (bi)carbonate species on Y_2O_3 in 10 mbar CO_2 up to 873 K under static conditions.
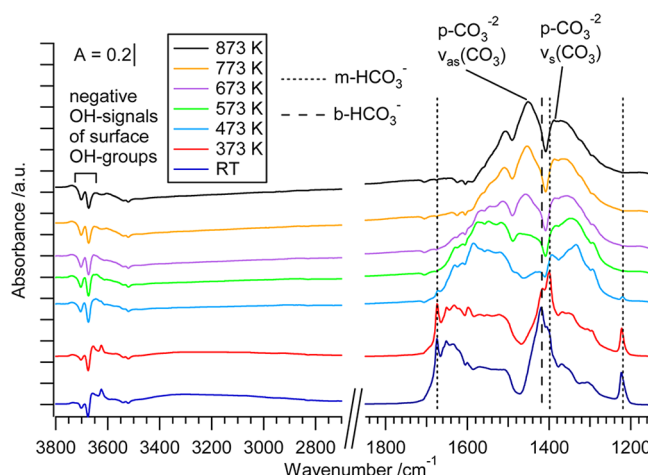

Figure 4. Infrared spectra collected on Y_2O_3 after exposure of 10 mbar static CO_2 upon heating to 873 K. Infrared spectra have been taken in 100 K steps. Important modes have been marked.

The bicarbonate species persist up to a temperature of 373 K, whereas the intensity of the peaks attributed to bidentate species decreases first. At 473 K the bicarbonates have vanished, and the remaining main species is the bridged carbonate, which subsequently is converted into polydentate carbonate species upon further temperature increase. Thus, at 873 K only signals of polydentate carbonate species are present. Hence, during heating the more weakly bound adsorbates are converted into more strongly bound carbonates. Summarizing, the process of this conversion, i.e., the binding strength of the different kinds of CO_2 adsorbates with increasing temperature on Y_2O_3, follows the sequence monodentate bicarbonate → bidentate bicarbonate → bridged carbonate → polydentate carbonate. Adsorbates on Y_2O_3, resulting from chemisorption of CO_2, can therefore not be removed entirely by heating up to 873 K. Additional experiments (not shown) show that a "carbonate-poisoned" Y_2O_3 surface can only be successfully recovered by heating in dry oxygen up to 873 K, likely because of efficient surface reoxidation.

A final comment on the spectroscopic requirements for studying carbonate formation on Y_2O_3 following CO_2 adsorption should be added. As Y_2O_3 is very prone to hydroxylation, even by traces of H_2O, carbonate formation is in turn highly favorable, but subsequent attribution to distinct carbonate species is not possible due to low resolution of the resulting spectra. This effect was observed in particular under "flowing CO_2" conditions, which under the chosen experimental conditions are less dry. Consequently, only static CO_2 adsorption under as dry as possible conditions, using a zeolite trap close to the IR cell for removing all traces of water from CO_2, permits collecting highly resolved carbonate spectra.

3.1.2. YSZ-8. Experiments on yttria-stabilized ZrO_2 (YSZ-8) under flowing conditions (CO_2 flow = 0.4 mL s^{-1}) show a behavior similar to pure Y_2O_3 at room temperature. In the case

of YSZ-8, flowing conditions were chosen to achieve more intense and thus more reliably interpretable signals because on YSZ-8 the carbonate adsorbates are generally more weakly bound as compared to on Y_2O_3. As apparent from Figure 5, showing also the thermal evolution of the carbonate species, the formation of Y_2O_3-analogous bi- and bridged carbonate species can also be observed.
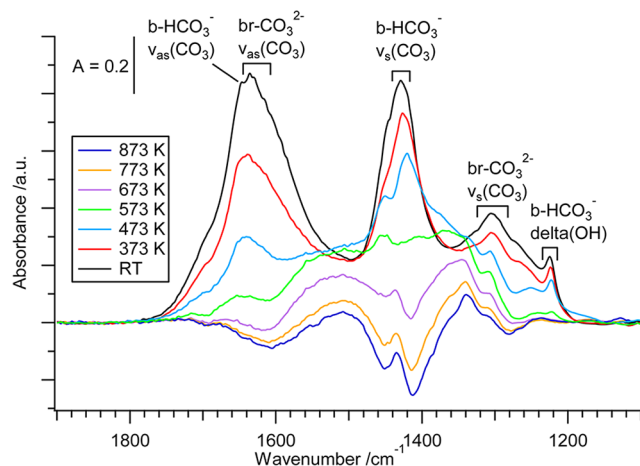

Figure 5. Infrared spectra collected during heating YSZ-8 in dry flowing CO_2 (CO_2 flow = 0.4 mL/s) up to 873 K together with the assignment of the observed (bi-) carbonates at room temperature.

The broad features located at 1305 cm^{-1} can be ascribed to the ν_s mode of the bridged carbonate, and the other main adsorbate signals at 1646, 1429, and 1225 cm^{-1} represent the corresponding bidentate carbonate. We note that the adsorption behavior of YSZ-8 very much resembles that of pure Y_2O_3 (cf. Figure 3) and is crucially different from spectra obtained on YSZ phases with a lower amount of Y, i.e., 3 mol %.[11] The latter is usually termed "tetragonal ZrO_2" in the literature and also adsorption-wise closely matches pure tetragonal ZrO_2.[12] In contrast to what was observed on pure Y_2O_3, (bi)carbonates on a YSZ-8 surface can be easily removed by heating, and almost no signals arising from polydentate carbonate species can be detected. Above a temperature of 573 K, these adsorbates decompose completely (Figure 5), although in this experiment flowing conditions with a pressure of 1 bar were chosen.

3.1.3. ZrO_2. On pure monoclinic ZrO_2, only very weak adsorption signals of CO_2 were observed after annealing in CO_2 pressures up to 12 mbar (Figure 6).

Static conditions with pressures below 12 mbar were enough to saturate the surface with chemisorbed species. Therefore, higher pressures or even flowing conditions do not intensify the very weak (bi)carbonate signals. Nevertheless, the vibrations at 1628, 1431, and 1223 cm^{-1} can be associated with a bicarbonate species on the surface. These signals very much coincide with literature-reported spectra taken on pure monoclinic ZrO_2.[11] However, in our case only very weak signals are observed, which is essentially due to the strong dehydroxylation treatment, conducted prior to the FT-IR measurements. Spectra shown in ref 11 (Figure 2 of that reference) clearly show peaks of surface hydroxyl groups, which are almost absent in our case. The starting pressure of 2 mbar at room temperature was enough to saturate the surface, and thus any further increase of the CO_2 pressure did not influence the
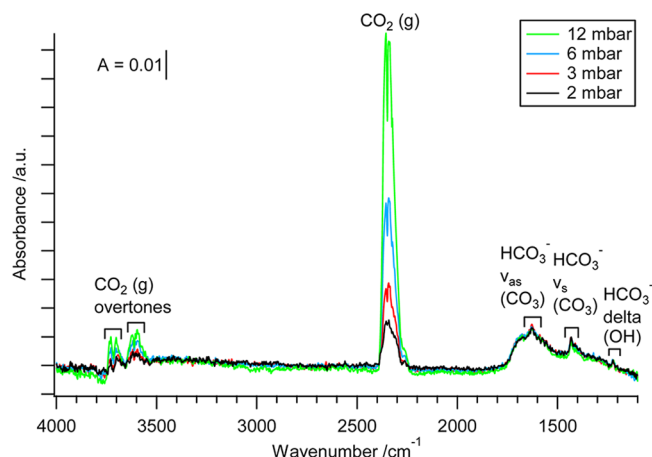

Figure 6. Infrared spectra taken after static adsorption of CO_2 on ZrO_2 at room temperature at pressures up to 12 mbar.

spectra. This corroborates the assumption that hydroxyl groups are of crucial importance for the chemisorption of CO_2. The following heating of ZrO_2 in CO_2 did not lead to reliably interpretable spectra due to the low signal-to-noise ratio.

3.1.4. Comparison of Y_2O_3, YSZ-8, and ZrO_2 upon CO_2 Adsorption. All oxides were pretreated by heating in air up to 1173 K, which leads to effective dehydroxylation of the surface. Only in the case of pure ZrO_2, no rehydroxylation was observed, even in the presence of water vapor at temperatures up to 873 K (see Figure S2, Supporting Information, also showing a comparison of the three oxides upon H_2O adsorption). As a result, ZrO_2 remains almost unreactive for CO_2 adsorption. This emphasizes the fact that surface hydroxyl species are important for effective chemisorption of CO_2.

The comparison of the three oxides Y_2O_3, YSZ-8, and ZrO_2 during exposure to CO_2 at room temperature and 873 K is highlighted in Figure 7 (concerning the assignment to (bi)carbonate species, see Table 1).

At room temperature, Y_2O_3 and YSZ-8 show a very similar behavior (with the exception of a different distribution of the (bi)carbonate species), suggesting that the hydroxylated yttrium centers in YSZ-8 are the reactive sites of the mixed oxide. Upon heating YSZ-8 to at least 673 K, the adsorbed carbonate species are completely removed, indicating weaker
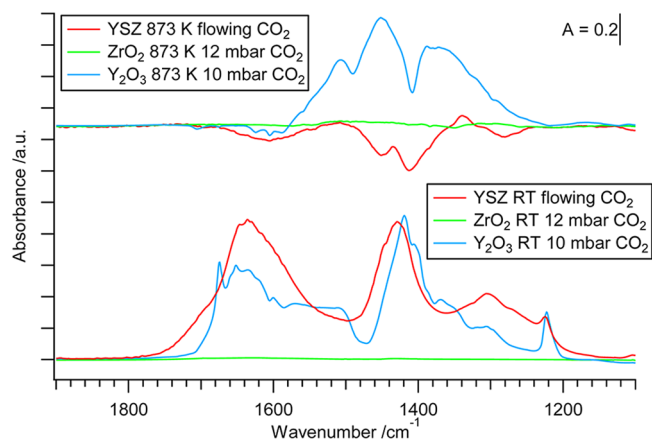

Figure 7. Comparison of the collected infrared spectra upon CO_2 adsorption at room temperature (lower panel) and 873 K (upper panel) on the surfaces of the oxides Y_2O_3, YSZ-8, and ZrO_2.

Table 1. Observed Wave Numbers and Assignment of the Peaks to (Bi-)carbonate Species Following CO_2 Adsorption on Y_2O_3, YSZ-8, and ZrO_2

oxide	carbonate species	$\nu_{as}(CO_3)$ [cm^{-1}]	$\nu_s(CO_3)$ [cm^{-1}]	$\delta(OH)$ [cm^{-1}]	$\nu(OH)$ [cm^{-1}]
Y_2O_3	monodentate bicarbonate	1674	1397	1223	3658
	bidentate bicarbonate	1652	1419	1223	3625
	bridged carbonate	1585	1334		
	poly dentate carbonate	1452	1388		
YSZ-8	bidentate bicarbonate	1646	1429	1225	not determined
	bridged carbonate	not determined	1305		
ZrO_2	bicarbonate	1628	1431	1223	

bonding than on pure Y_2O_3, which is also reflected by the eventual absence of strongly bound polydentate carbonate species. As a conclusion from measurements on pure Y_2O_3, the monodentate bicarbonate must be more strongly bound than the bidentate carbonate, and the conversion to the associated bridged species—bound to two yttrium atoms—is the essential step toward even more strongly bound species, which are hard to remove. Most likely, the monodentate bicarbonate is not only bound to an yttrium atom via one of its oxygen atoms but also stabilized through a hydrogen bond with a neighboring hydroxyl group. In contrast, YSZ-8 obviously does not exhibit these neighboring Y_2O_3 centers. If water binds dissociatively onto a defect caused by a Y^{3+} in the ZrO_2 lattice, a HO^- bound to the yttrium (because of its basicity) is formed. This is the adsorption site for a CO_2 molecule to subsequently form a (bi-)carbonate species. In the case of a bridged carbonate, this species is more likely bound to a yttrium and a zirconium atom than to two adjacent Y^{3+} centers, and this seems to make the difference in the binding strength of this particular species. Comparing the carbonate spectra provided by Pokrovski et al.[12] and Baeza et al.[11] obtained on different hydroxylated ZrO_2 polymorphs, we note remarkable similarities in the overall features of the carbonate regions but a slightly different population of the different (bi)carbonate species. On pure Y_2O_3, the bicarbonate species are dominating, whereas on YSZ-8, the relative fraction of bidentate and bridged carbonate species is higher. In close correlation, the spectra of Pokrovski et al. show a higher fraction of bridged species. Most important, the spectra obtained on tetragonal ZrO_2 are strikingly different from those observed on YSZ-8. The main species on tetragonal ZrO_2, as reported by Baeza et al.[11] and Pokrovski et al.,[12] are polydentate carbonate species already after adsorption at room temperature (cf. Figure 3 of ref 12). However, despite the different distribution of bicarbonate, bidentate, and bridged carbonates, no polydentate carbonates are found on YSZ-8, further confirming that the adsorption of YSZ is basically dominated by the hydroxylated Y centers.

3.2. CO Adsorption. Besides molecular adsorption as "intact" CO, for the adsorption of a CO molecule and following reaction to CO_2 on an oxide surface, two mechanisms are in principle possible:[14,21] (i) the CO molecule reacts with an oxygen atom of the lattice to form CO_2 and leaves an oxygen vacancy behind or (ii) it inserts into a surface hydroxyl group, forms a formate, and this intermediate subsequently decomposes into CO_2 (or reacts backward to CO and OH). Figure S3 (Supporting Information) shows the possible formate species on an oxide surface.

3.2.1. Y_2O_3. Figure 8 shows Y_2O_3 heated in 290 mbar CO under static measurement conditions (main panel).

At room temperature, no adsorption or reaction takes place, but during heating, CO_2 formation starts at 373 K. As an
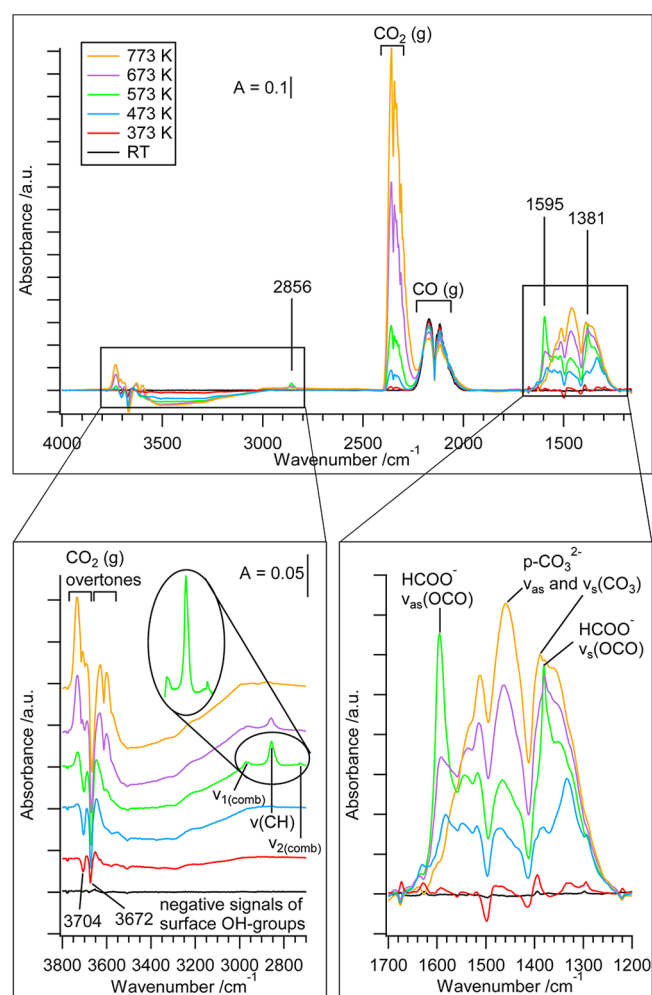
Figure 8. Infrared spectra taken upon heating Y_2O_3 in 290 mbar CO under static measurement conditions up to 773 K (upper panel) and with details of the wavenumber region above 2700 cm^{-1} (right lower panel) and below 1700 cm^{-1} (left lower panel).

intermediate of this reaction, signals of formates can be detected, with an intensity maximum reached at 573 K. The corresponding vibrations for the ν_{as} and the ν_s mode of the formate are at 1595 and 1381 cm^{-1}, and the related $\nu(CH)$ vibration is located at 2856 cm^{-1}. Also the decrease of surface hydroxyl groups (left lower panel) can be detected starting from a temperature of 373 K at 3704 and 3672 cm^{-1}, which illustrates the analogy to the above-mentioned observations regarding CO_2 adsorption/carbonate formation. Above a temperature of 573 K the formates are rapidly decomposed. Because of the formation of CO_2, vibration modes for carbonates are observed as well—especially in analogy to the

measurements in CO_2 at 473 K the bridged carbonate is the main species. At 773 K the polydentate carbonate is again predominant (right lower panel). Accompanied by the already mentioned formate signals, combination modes, namely, $\nu_{1(combi)}$ ($\nu_{as}(CO_2 + \delta(CH))$ at 2972 cm^{-1} and $\nu_{2(combi)}$ ($\nu_s(CO_2) + \delta(CH)$) at 2727 cm^{-1}, are observed (lower left panel).[18,21] On the basis of refs 18 and 21 the observed formate species are assigned to a bidentate or bridged species.

Starting from room temperature, weak signals are observed at 1630 and 1294 cm^{-1}, which may be arising from monodentate formate species. Comparing our results to those of the literature,[19−21] it is generally assumed that the monodentate species is the more reactive and less stable one. Therefore, the bidentate or bridged formate species could be mainly a spectator below 773 K.

3.2.2. YSZ-8. Figure 9 shows YSZ-8 heated in flowing CO (CO flow = 0.2 mL s^{-1}).
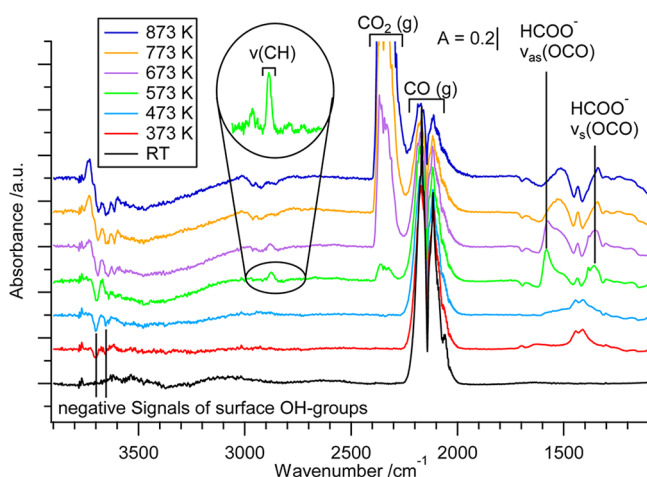

Figure 9. Infrared spectra collected upon heating YSZ-8 in flowing CO (CO flow = 0.2 mL s^{-1}) up to 873 K. Infrared spectra have been taken in 100 K steps.

As for CO_2, flowing conditions were chosen for YSZ-8 because of better interpretable spectra due to increased adsorption of surface species. At room temperature, no signals of any adsorbed molecules are detected. However, the processes on YSZ-8 are again quite similar to those observed on Y_2O_3, with the exception that the spectra are more easy to interpret because of no disturbing (bi)carbonates. CO_2 formation starts at 573 K, and in-parallel typical formate peaks at 2875 cm^{-1} for the $\nu(CH)$ mode and 1581, 1384, and 1357 cm^{-1} representing the $\nu_{as}(OCO)$, the $\delta(CH)$, and the $\nu_{as}(OCO)$ mode of the formate arise. The combination modes are less pronounced as compared to Y_2O_3. These formate vibration modes are visible up to a temperature of 675 K, and above 773 K the same spectra fingerprint as for CO_2 adsorption is observed. In other words, no adsorbates are detected anymore. During heating, also a decrease of signals at 3690, 3643, and 3613 cm^{-1}, attributed to surface hydroxyl groups, occurs. Interestingly, on YSZ-8 no signals for monodentate formate species are visible.

3.2.3. ZrO_2. To ensure full correlation with the CO_2 measurements, static conditions are again chosen. Also by analogy to CO_2 adsorption, pure dehydroxylated ZrO_2 did not show significant signals attributable to surface adsorbates in static CO (Figure 10).
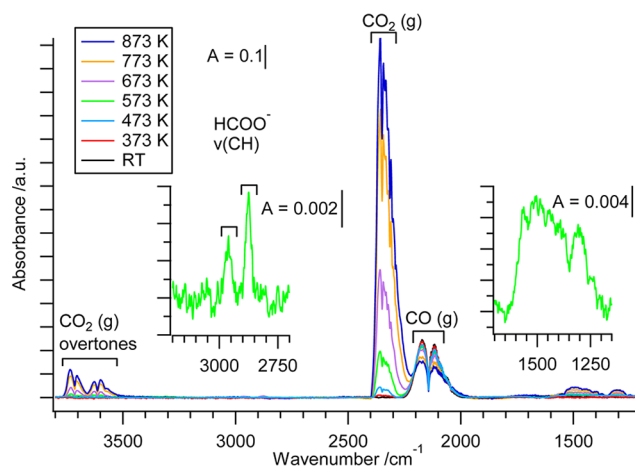

Figure 10. Infrared spectra collected upon heating ZrO_2 following static adsorption of 248 mbar CO up to 873 K. Infrared spectra have been taken in 100 K steps.

This essentially verifies that no defects (which are usually titrated by molecular CO adsorption[7]) and no substantial amount of hydroxyl groups are present because of the oxidizing high-temperature pretreatment of the sample. However, during heating in 248 mbar CO at 573 K, very weak peaks at 2361 and 2875 cm^{-1} being attributable to $\nu(CH)$ and/or combination modes of formates are observed (see left inset). The associated broad signals in the region below 1600 cm^{-1} are too weak for an appropriate interpretation. We note that all oxides were pretreated by heating up to 1173 K in air to reduce impurities, and in the case of ZrO_2 no rehydroxylation takes place. Because of the lack of surface hydroxyl groups only a minute amount of formates can in turn be formed.

3.2.4. Comparison of Y_2O_3, YSZ-8, and ZrO_2 Regarding CO Adsorption. The comparison of the adsorption behavior during exposure to CO at maximum formate signal, namely, at 573 K, is highlighted in Figure 11.
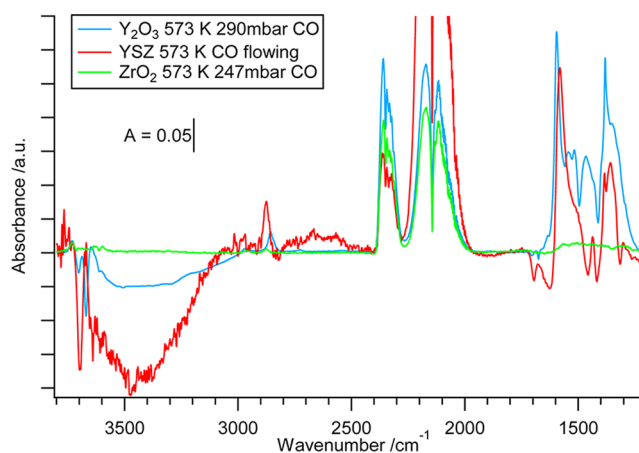

Figure 11. Comparison of the infrared spectra of the oxides Y_2O_3, YSZ-8, and ZrO_2 at maximum formate signal (573 K).

On none of the three studied oxides were signals of adsorbed (physisorbed) CO detected, as was previously shown for more defective ZrO_2 samples.[10] We might anticipate that all defects are therefore quenched upon the preannealing in oxygen to 1173 K. Note that our results strongly suggest that in line with the initial question about the mechanism of CO_2 formation

following CO adsorption a mechanism including the participation of surface OH-groups is found to be most likely prevailing (mechanism ii). Substantial reduction of the oxides is therefore less likely, and this assumption is also corroborated by additional electric impedance measurements, which only show the reversible formation of thermally excited charge carriers but no substantial formation of surface defects (Figure S4, Supporting Information).

Table 2 summarizes the main formate vibration modes observed on all oxides.

Table 2. Observed Wave Numbers and Assignment of the Peaks to Formate Species Following CO Adsorption of Y_2O_3, YSZ-8, and ZrO_2

oxide	ν_{as} [cm^{-1}]	ν_s [cm^{-1}]	$\nu(CH)$ [cm^{-1}]
Y_2O_3	1595	1381	2856
YSZ-8	1581	1357	2875
ZrO_2	not determined	not determined	2875

Like in the case of CO_2 adsorption, the comparison of the oxides shows that the yttrium amount in YSZ-8 is important for chemisorption reactivity because in contrast to pure ZrO_2 the surface of the mixed oxide can be easily reactivated after dehydroxylation. This again corroborates the assumption that the basic surface hydroxyl species on Y-centers are also important for the conversion of CO toward formates. On YSZ-8, the carbonates—resulting from adsorption of the formed CO_2—are not bound as strongly as on Y_2O_3 and thus do not interfere with the formates.

4. CONCLUSION

Using FT-IR spectroscopy investigations, surface reaction-induced adsorbates of CO_2 and CO on the technically relevant oxides Y_2O_3, YSZ-8, and ZrO_2 could be identified. Y_2O_3 and YSZ-8 show much higher reactivity toward both CO_2 and CO adsorption than ZrO_2. The reversible formation and basic presence of surface hydroxyl groups is a crucial factor of an active surface, and the yttrium centers in YSZ-8 seem to essentially exhibit this quality. Thus, they are the C1-reactive sites of the mixed oxide YSZ-8. On Y_2O_3 and YSZ-8, several kinds of carbonates are detected, whereby in general on Y_2O_3 the adsorbates are more difficult to remove because of obviously easier conversion to more strongly bound, higher-coordinated species. The mechanism of chemisorption of CO_2 most likely proceeds via an insertion of the CO_2 molecule into a surface hydroxyl group and the following formation of a bicarbonate. Further conversion into more strongly bound carbonate species is observed at higher temperatures. In the case of CO oxidation the formation of formate intermediates is observed on all oxides, but the absence of a significant amount of hydroxyl groups on ZrO_2 leads to very weak signals on this oxide. The present FT-IR spectroscopic study moreover suggests that SOFC-related C1 reactions (water–gas shift reaction, intermediates of CH_4 reforming) on YSZ-based cermet anodes may be mechanistically/kinetically influenced by the basic character and by the pronounced reversibility and degree of hydroxylation of the Y-centers in YSZ-8.

ASSOCIATED CONTENT

S **Supporting Information**

S1: Structure of possible (bi)carbonate species on the surface of an oxide (adapted from ref 15). S2: IR spectra collected on the three oxides upon adsorption of $H_2O(g)$. Pressures include 21 mbar H_2O for Y_2O_3 and ZrO_2 and 24 mbar for YSZ. **S3:** Structure of possible formate species on the surface of an oxide (adapted from ref 21). **S4:** Comparison of the three oxides by electric impedance measurements in flowing CO, heated to 1073 K. This material is available free of charge via the Internet at http://pubs.acs.org.

AUTHOR INFORMATION

Corresponding Author

*Tel.: 00435125075056. Fax: 00435125075056. E-mail: simon.penner@uibk.ac.at.

Notes

The authors declare no competing financial interest.

REFERENCES

(1) Takahashi, H.; Takeguchi, T.; Yamamoto, N.; Matsuda, M.; Kobayashi, E.; Ueda, W. Effect of Interaction between Ni and YSZ on Coke Deposition During Steam Reforming of Methane on Ni/YSZ Anode Catalysts for an IR-SOFC. *J. Mol. Catal. A* **2011**, *350* (1−2), 69−74.

(2) Viazzi, C.; Bonino, J. P.; Ansart, F.; Barnabe, A. Structural Study of Metastable Tetragonal YSZ Powders Produced via a Sol-gel Route. *J. Alloys Compd.* **2008**, *452* (2), 377−383.

(3) Dombrovsky, L. A.; Rousseau, B.; Echegut, P.; Randrianalisoa, J. H.; Baillis, D. High Temperature Infrared Properties of YSZ Electrolyte Ceramics for SOFCs: Experimental Determination and Theoretical Modeling. *J. Am. Ceram. Soc.* **2011**, *94* (12), 4310−4316.

(4) Liu, D. W.; Perry, C. H.; Ingel, R. P. Infrared-Spectra in Nonstoichiometric Yttria-Stabilized Zirconia Mixed-Crystals at Elevated Temperatures. *J. Appl. Phys.* **1988**, *64* (3), 1413−1417.

(5) Heshmatpour, F.; Khodaiy, Z.; Aghakhanpour, R. B. Synthesis and Characterization of Pure Tetragonal Nanocrystalline Sulfated 8YSZ Powder by Sol-gel Route. *Powder Technol.* **2012**, *224*, 12−18.

(6) Dulaurent, O.; Bianchi, D. Adsorption Model and Heats of Adsorption for Linear CO Species Adsorbed on ZrO_2 and Pt/ZrO_2 Using FTIR Spectroscopy. *Appl. Catal., A* **2001**, *207* (1−2), 211−219.

(7) Ryczkowski, J. IR Spectroscopy in Catalysis. *Catal. Today* **2001**, *68* (4), 263−381.

(8) Kantcheva, M.; Milanova, M.; Avramova, I.; Mametsheripov, S. Spectroscopic Characterization of Gold Supported on Tungstated Zirconia. *Catal. Today* **2012**, *187* (1), 39−47.

(9) Goscianska, J.; Ziolek, M.; Gibson, E.; Daturi, M. Novel Mesoporous Zirconia-Based Catalysts for WGS Reaction. *Appl. Catal., B* **2010**, *97* (1−2), 49−56.

(10) Bolis, V.; Magnacca, G.; Cerrato, G.; Morterra, C. Effect of Sulfation on the Acid-Base Properties of Tetragonal Zirconia. A Calorimetric and IR Spectroscopic Study. *Top. Catal.* **2002**, *19* (3−4), 259−269.

(11) Bachiller-Baeza, B.; Rodriguez-Ramos, I.; Guerrero-Ruiz, A. Interaction of Carbon Dioxide with the Surface of Zirconia Polymorphs. *Langmuir* **1998**, *14* (13), 3556−3564.

(12) Pokrovski, K.; Jung, K. T.; Bell, A. T. Investigation of CO and CO_2 Adsorption on Tetragonal and Monoclinic Zirconia. *Langmuir* **2001**, *17* (14), 4297−4303.

(13) Ma, Z.; Yang, C.; Wei, W.; Li, W.; Sun, Y. Surface Properties and CO Adsorption on Zirconia Polymorphs. *J. Mol. Catal. A* **2005**, *227*, 119−124.

(14) Silva, A. M.; Barandas, A.; Costa, L. O. O.; Borges, L. E. P.; Mattos, L. V.; Noronha, F. B. Partial Oxidation of Ethanol on Ru/Y_2O_3

and Pd/Y$_2$O$_3$ Catalysts for Hydrogen Production. *Catal. Today* **2007**, *129* (3−4), 297−304.

(15) Collins, S. E.; Baltanas, M. A.; Bonivardi, A. L. Infrared Spectroscopic Study of the Carbon Dioxide Adsorption on the Surface of Ga$_2$O$_3$ Polymorphs. *J. Phys. Chem. B* **2006**, *110* (11), 5498−5507.

(16) Bianchi, D.; Gass, J. L.; Khalfallah, M.; Teichner, S. J. Intermediate Species on Zirconia Supported Methanol Aerogel Catalysts. 1. State of the Catalyst Surface Before and After the Adsorption of Hydrogen. *Appl. Catal., A* **1993**, *101* (2), 297−315.

(17) Binet, C.; Daturi, M.; Lavalley, J. C. IR Study of Polycrystalline Ceria Properties in Oxidised and Reduced States. *Catal. Today* **1999**, *50* (2), 207−225.

(18) Collins, S. E.; Baltanas, M. A.; Bonivardi, A. L. An Infrared Study of the Intermediates of Methanol Synthesis from Carbon Dioxide over Pd/β-Ga$_2$O$_3$. *J. Catal.* **2004**, *226* (2), 410−421.

(19) Haghofer, A.; Ferri, D.; Fottinger, K.; Rupprechter, G. Who Is Doing the Job? Unraveling the Role of Ga$_2$O$_3$ in Methanol Steam Reforming on Pd$_2$Ga/Ga$_2$O$_3$. *ACS Catal.* **2012**, *2* (11), 2305−2315.

(20) Vayssilov, G. N.; Mihaylov, M., St; Petkov, P.; Hadjiivanov, K. I.; Neyman, K. M. Reassignment of the Vibrational Spectra of Carbonates, Formates, and Related Surface Species on Ceria: A Combined Density Functional and Infrared Spectroscopy Investigation. *J. Phys. Chem. C* **2011**, *115* (47), 23435−23454.

(21) Calatayud, M.; Collins, S. E.; Baltanas, M. A.; Bonivardi, A. L. Stability of Formate Species on β-Ga$_2$O$_3$. *Phys. Chem. Chem. Phys.* **2009**, *11* (9), 1397−1405.

17673

dx.doi.org/10.1021/jp405625x | *J. Phys. Chem. C* 2013, 117, 17666−17673